Electronic Supplementary Material (ESI) for Lab on a Chip.

Supporting Information for

A Microfluidic Impedance Cytometry with Flat-end Cylindrical Electrodes for Accurate and Fast Analysis of Marine Microalgae

Xiaoming Chen,*[a, b] Mo Shen,[a, b] Shun Liu,[a, b] Chungang Wu,[a, b] Liangliang Sun,[a, b] Zhipeng Song,[a, b] Jishun Shi,[a, b] Yulong Yuan,[a, b] and Yong Zhao*[a, b]

[a]*School of Control Engineering, Northeastern University at Qinhuangdao, Qinhuangdao 066004, PR China. E-mail: chenxiaoming@neuq.edu.cn*
[b]*Hebei Key Laboratory of Micro-Nano Precision Optical Sensing and Measurement Technology, Qinhuangdao, 066004, PR China. E-mail: zhaoyong@ise.neu.edu.cn.*

Section 1: Method of numerical simulation

We conducted the numerical simulation using the software of Comsol Multiphysics 6.0. We firstly established the simulation model, and the flat-end cylindrical electrodes were equivalent to two circle surfaces on the both sides of the fluid domain. The microalgae were equivalent to 3D spindle. We selected the module of Electric Currents to investigate the impedance change of microalgae when they travel through the detection zone. The left flat-end cylindrical electrode was employed an excited voltage as the terminal with the amplitude

$$V = V_0 \tag{S1}$$

The right flat-end electrode was grounded with the amplitude of

$$V = 0 \tag{S2}$$

The surfaces of the microalgae were employed the contact impedance

$$n \cdot J_1 = \frac{1}{d_s}(\sigma + j\omega\varepsilon_0\varepsilon_r)(V_1 - V_2) \tag{S3}$$

$$n \cdot J_2 = \frac{1}{d_s}(\sigma + j\omega\varepsilon_0\varepsilon_r)(V_2 - V_1) \tag{S4}$$

The fluid in the detection zone was required to comply with current conservation:

$$\nabla \cdot J = Q_{j,V} \tag{S5}$$

$$J = \sigma E + j\omega D + J_e \tag{S6}$$

$$E = -\nabla V \tag{S7}$$

The initial potential of the detection zone is set to

$$V_{initial} = 0 \tag{S8}$$

We choose the frequency domain to investigate the impedance of the microalgal cells. According to the computation results, we input the equation of cell impedance and take the position of cell along X coordinate as sweep parameters. In this way, we can simulate the change of cell impedance in the dynamic detection. We changed the distance between microalgae and detection zone center in the microchannel to simulate the travel process of microalgae in the detection.

Table S1 Physical and geometrical parameters in numerical simulation.

Parameters	Value	Implication
L	400 µm	Length of detection channel
W	40 µm	Width of detection channel
H	81 µm	Height of detection channel
R	40 µm	Radius of the flat end electrode
R_c	3.4 µm	Radius of microalgae
L_c	36 µm	Length of microalgae

σ_m	0.2 S/m	Conductivity of the solution
ε_m	80	Relative permittivity of the solution
ρ_m	1000 kg/m^3	Density of the solution
μ	0.0000055	Dynamic viscosity of the solution
ε_c	60	Relative permittivity of the cells
σ_c	0.65	Conductivity of the cells
ρ_c	1000 kg/m^3	Density of the cells
φ	0~1	Volume fraction of cells
k	80~200	Cell constant
D	36 µm	Effective size of cells

Section 2: Impedance signals of different-size cells

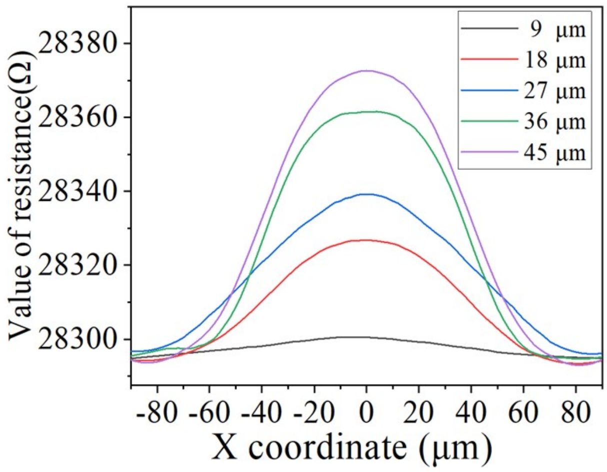

Figure.S1 Impedance signals of different-size cells.

Section 3: Flow distribution with and without the space in the wire channel

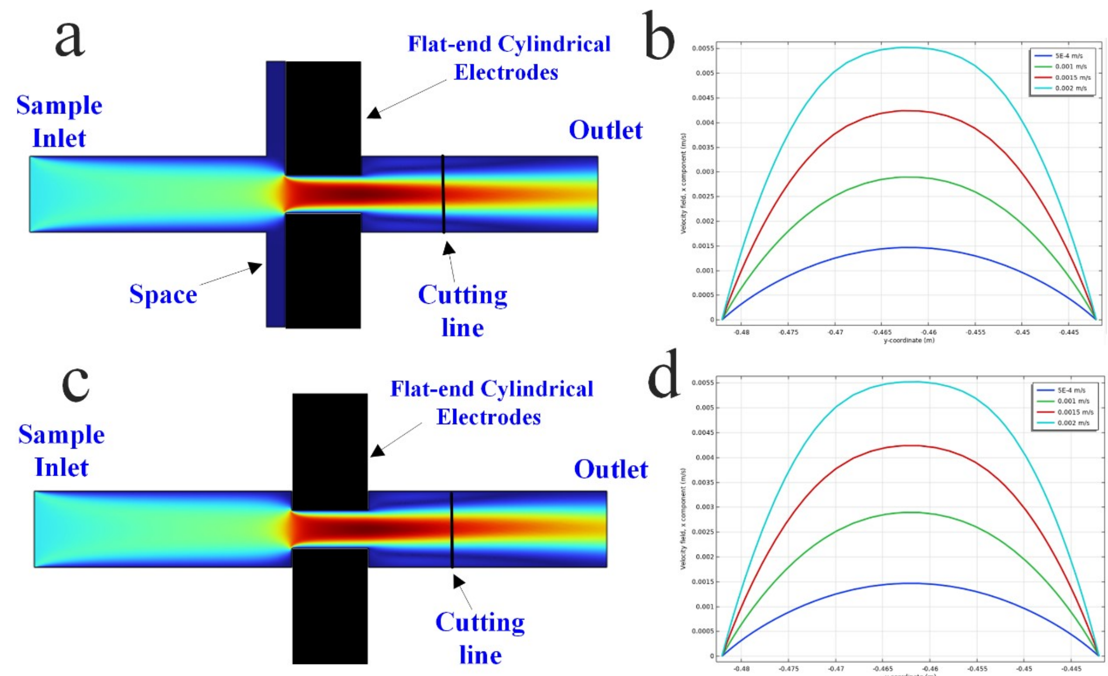

Figure.S2 Numerical simulation to investigate the effect of wire channel space on the flow distribution. (a/c) Flow field distribution in the detection zone with/ without wire channel space. (b/d) Velocity of fluid along X coordinate in the detection zone with/ without wire channel space.

Section 4: Impedance signals of *Haematococcus pluvialis* under different ion concentration

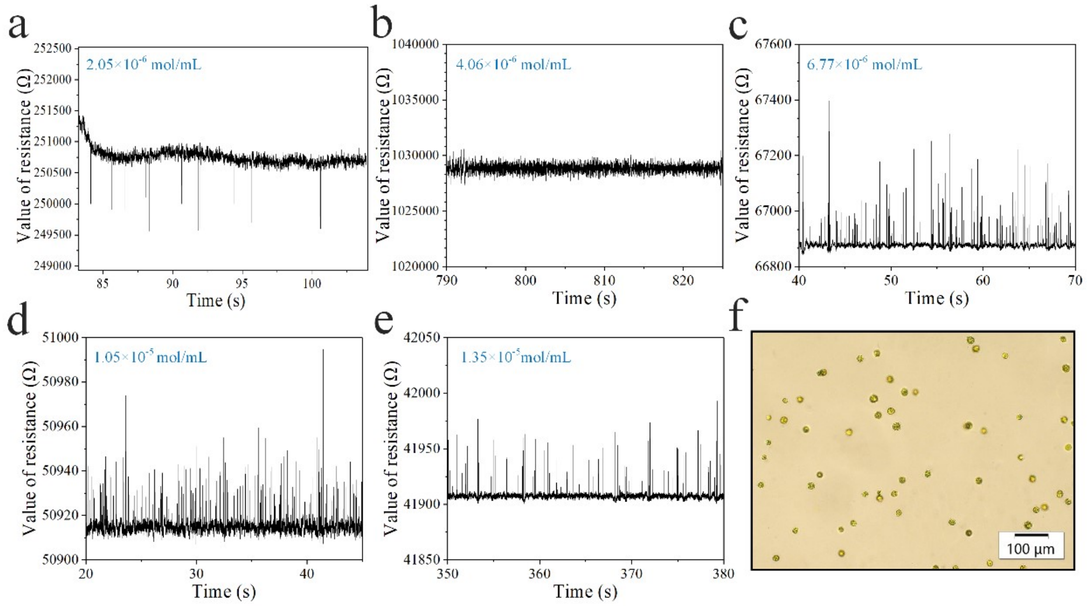

Figure.S3 Impedance signals of *Haematococcus pluvialis* under different ion concentrations. (a) $2.05x10^{-6}$ mol/mL. (b) $4.06x10^{-6}$ mol/mL. (c) $6.77x10^{-6}$ mol/mL. (d) $1.05x10^{-5}$ mol/mL. (e) $1.35x10^{-5}$ mol/mL. (f) Micrograph of *Haematococcus pluvialis*.

Section 5: Micrographs of *Euglena* cells under different ion concentrations

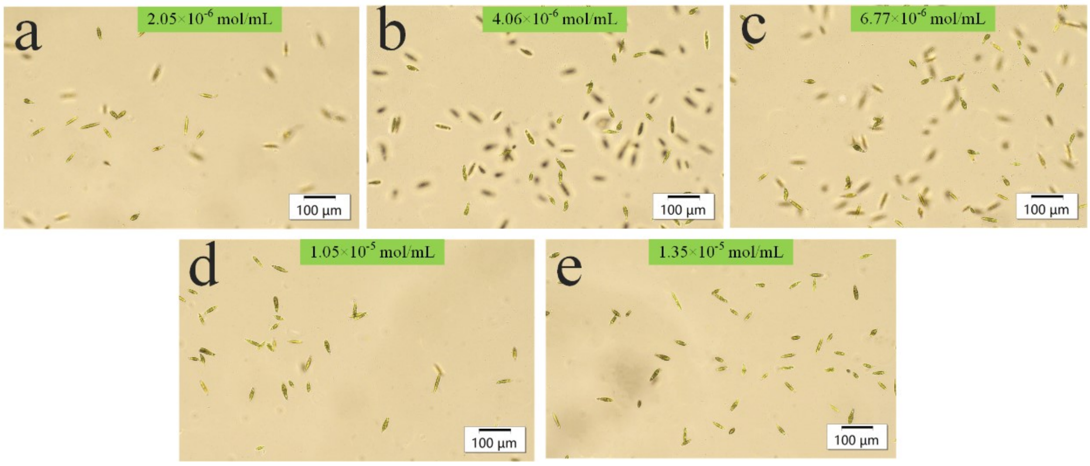

Figure.S4 Micrographs of *Euglena* under different ion concentrations. (a) 2.05×10^{-6} mol/mL. (b) 4.06×10^{-6} mol/mL. (c) 6.77×10^{-6} mol/mL. (d) 1.05×10^{-5} mol/mL. (e) 1.35×10^{-5} mol/mL.

Section 6: Impedance signals of *Haematococcus pluvialis* under different voltages

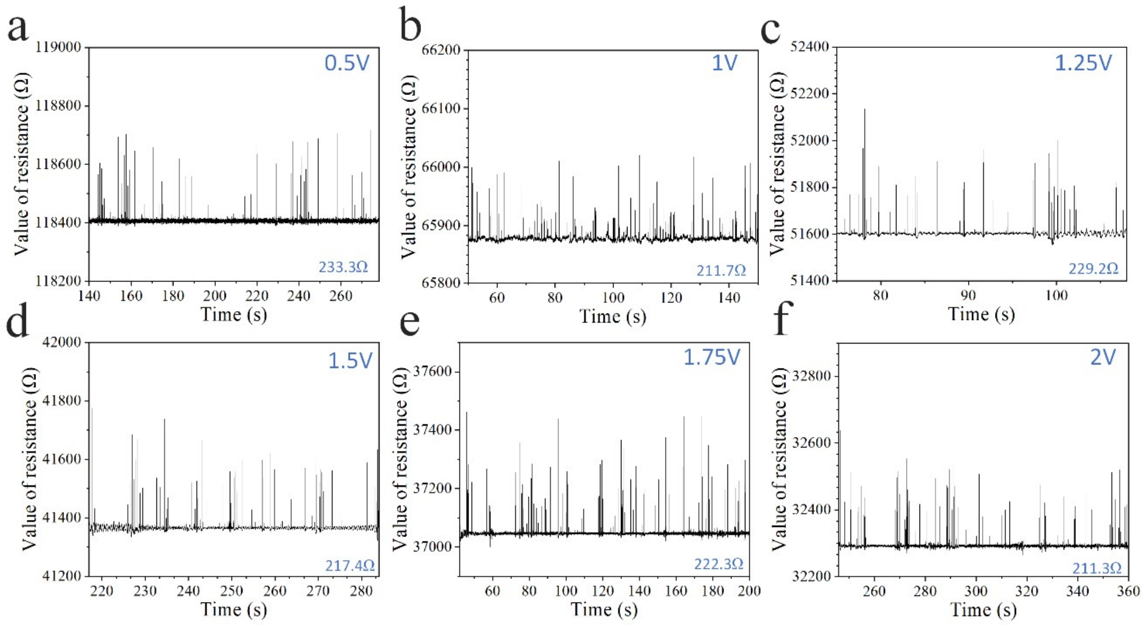

Figure.S5 Impedance of Haematococcus pluvialis under different applied voltages. (a) *A*=0.5 V. (b) *A*=1 V. (c) *A*=1.25 V. (d) *A*=1.5 V. (e) *A*=1.75 V. (f) *A*=2 V.

Section 7: Impedance signals of *Haematococcus pluvialis* at different cell density

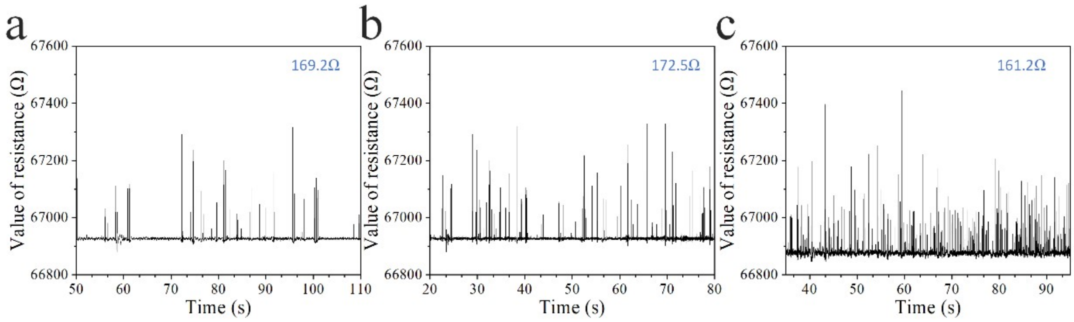

Figure S6 Impedances of *Haematococcus pluvialis* at different concentration. (a) 100 cells/µL. (b) 200 cells/µL. (c) 400 cells/µL.

Section 8: Impedance signals of *Haematococcus pluvialis* in the microfluidic impedance cytometry with different electrode gap

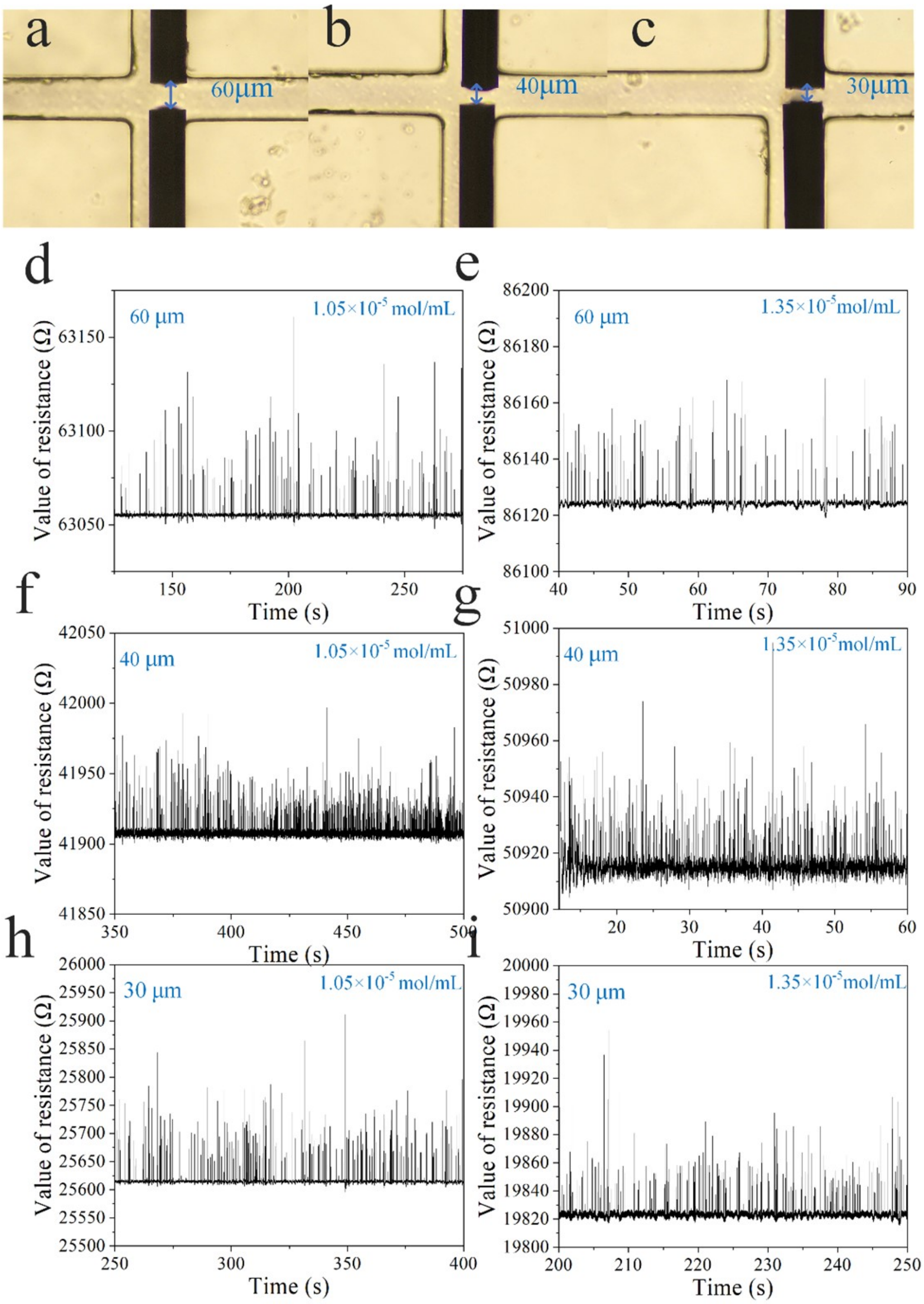

Figure.S7 Influence of electrode gap on the impedance signals of microalgae. (a-c) Micrograph of the detection zone in the device with electrode gap of 60 μm, 40 μm and 30 μm. (d-f) Impedance signals of *Haematococcus pluvialis* detected in three devices at the ion concentration of 1.05×10^{-5} mol/mL. (g-i) Impedance signals of *Haematococcus pluvialis* detected in three devices at the ion concentration of 1.35×10^{-5} mol/mL.

Section 9: Comparation with other microfluidic impedance cytometry systems for detection of microalgae

Table S2 Comparation with other microfluidic impedance cytometry systems for detection of microalgae

Electrode structure	Materials of electrodes	Fabrication of electrodes	Throughput	Applied species	Reference
Planar electrode	Cr/Au electrodes	Sputtering and standard photolithography techniques	900 cells/s	*Euglena*	Reference[1]
Planar electrode	Cr/Au electrodes	Sputtering and standard photolithography techniques	--	*Euglena*	Reference [2]
Planar electrode	Cr/Au electrodes	Sputtering and standard photolithography techniques	1500 cells/s	*Euglena*	Reference [3]
Planar electrode	Cr/Au electrodes	Sputtering and standard photolithography techniques	--	*Euglena*	Reference [4]
Planar eletrode	Au electrodes	Sputtering and standard photolithography techniques	--	*Picochlorum SE3*	Reference [5]
Planar eletrode	Ti:Au:Ti	Sputtering and standard photolithography techniques	--	*Isochrysis galbana, Synechococcus sp. Rhodosorus m.*	Reference [6]
Planar eletrode	tantalum/platinum	--	--	*Emiliania huxleyi*	Reference [7]
3D electrode	Copper electrodes	--	--	*D. Salina*	Reference [8]
Flat-end cylindrical electrode	Stainless steel wires	Grinding process	1800 cells/s	*Haematococcus pluvialis Euglena Oocystis sp*	This work

Section 10: Detection of *Haematococcus pluvialis* using PBS solution

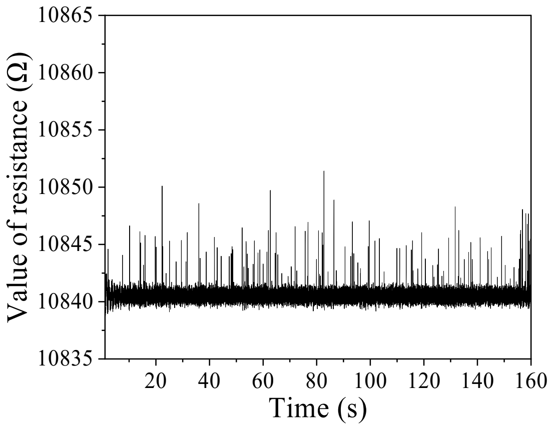

Figure.S8 Impedance signals of *Haematococcus pluvialis* in the PBS solution.

Section 11: Detection of *Haematococcus pluvialis*

Video S1 Impedance signals of *Haematococcus pluvialis* at A=1 V, f=500 kHz and Q=10 μL/min.

Reference

1. T. Tang, X. Liu, Y. Yuan, R. Kiya, Y. Shen, T. Zhang, K. Suzuki, Y. Tanaka, M. Li, Y. Hosokawa and Y. Yalikun, *Lab on a chip*, 2022, **22**, 550-559.
2. T. Tang, X. Liu, R. Kiya, Y. Shen, Y. Yuan, T. Zhang, K. Suzuki, Y. Tanaka, M. Li, Y. Hosokawa and Y. Yalikun, *Biosensors and bioelectronics* 2021, **193**.
3. T. Tang, X. Liu, Y. Yuan, T. Zhang, R. Kiya, K. Suzuki, Y. Tanaka, M. Li, Y. Hosokawa and Y. Yalikun, *Sensors and Actuators B: Chemical*, 2022, **358**.
4. T. Tang, X. Liu, Y. Yuan, T. Zhang, R. Kiya, Y. Yang, K. Suzuki, Y. Tanaka, M. Li, Y. Hosokawa and Y. Yalikun, *Microsyst nanoeng* 2022, **8**, 68.
5. J. Sui, F. Foflonker, D. Bhattacharya and M. Javanmard, *Sci rep* 2020, **10**, 1251.
6. G. Benazzi, D. Holmes, T. Sun, M. C. Mowlem and H. Morgan, *IET Nanobiotechnol*, 2007, **1**, 94-101.
7. D. S. de Bruijn, P. M. Ter Braak, D. B. Van de Waal, W. Olthuis and A. van den Berg, *Biosens bioelectron* 2020, **173**, 112808.
8. Y. X. Song, M. Q. Li, J. D. Yang, J. S. Wang, X. X. Pan, Y. Q. Sun and D. Q. Li, *Sensors and actuators b-chemical* 2014, **194**, 164-172.